Chinese Journal of Physics 59 (2019) 138–152

Contents lists available at ScienceDirect

Chinese Journal of Physics

journal homepage: www.elsevier.com/locate/cjph

A novel parameter-induced adaptive stochastic resonance system based on composite multi-stable potential model

Jiao Shangbin*, Qiao Xiaoxue, Lei Shuang, Jiang Wei

Shaanxi Key Laboratory of Complex System Control and Intelligent Information Processing, Xi'an University of Technology, Xi'an 710048, China

ARTICLE INFO

Keywords:
Stochastic resonance
Composite multi-stable model
Weak signal detection
Collaborative optimization of multiple parameters
Differential brain storm optimization algorithm

ABSTRACT

Stochastic resonance (SR) is used widely as a weak signal detection method by using noise in many fields. In order to improve the weak signal processing capability of SR, a novel composite multi-stable model is proposed, which is constructed by the joint of the tristable model and the Gaussian Potential (GP) model. The SR system based on this model is constructed and the signal-to-noise ratio (SNR) is regarded as the index to measure the SR effect. The differential brain storm optimization (DBSO) algorithm is used to optimize the system parameters collaboratively to achieve parameter-induced adaptive SR. The influences of the system parameters V and R and the noise intensity D on the output response of SR system are analyzed under Gaussian white noise and α stable noise environments, and the advantages of the composite multi-stable SR system over the traditional tristable system are verified. For different levels of weak signals, the output performances of SR systems based on composite multi-stable model, traditional tristable model, composite tristable model are compared and analyzed. The results prove that the proposed model has better performance. Meanwhile, the adaptive detection of the multiple high-frequency weak signal is realized using the composite multi-stable SR system. The simulation results show that the proposed system has strong weak signal processing capability and good immunity to noise types, which widens the application range of SR in practical engineering.

1. Introduction

Stochastic resonance (SR) has received extensive attention from scholars since it was proposed by Benzi et al. in 1981, and has been applied in many fields [1–6]. In the field of weak signal detection, SR is a kind of noise-assisted or enhanced weak signal detection method, which is induced by the synergy of the nonlinear system (potential well force), noise (stochastic force) and input signal (periodic force) [7,8]. Compared with other weak signal detection methods, SR uses noise instead of suppressing it. The partial energy of the noise can be transformed into the signal energy via a nonlinear potential function, thereby realizing the enhancement and detection of weak characteristic signals [9,10].

In the SR system, the structure of the potential model has an important influence on the detection effect of weak signals. Many research results based on the classical bistable and monostable SR models have been obtained [11–15]. In recent years, the tristable SR system has been studied extensively [16–21]. The literature [20] shows that the tristable model can improve the output SNR and detect weak signals with lower input signal-to-noise ratio (SNR), compared with the traditional bistable and monostable models. The results of the literature [21] also show that the detection effect of the tristable SR system is better than the bistable system. In fact, there are some cases where the noise random force and the signal periodic force are exceedingly weak in industrial measurement. In

* Corresponding author.
E-mail address: jiaoshangbin@xaut.edu.cn (S. Jiao).

https://doi.org/10.1016/j.cjph.2019.02.031
Received 13 September 2018; Received in revised form 19 February 2019; Accepted 23 February 2019
Available online 27 February 2019

this case, no matter using the bistable or tristable models, it is difficult for the particles to cross the barrier from one potential well to another by adjusting system parameters, and the limited noise energy cannot be converted into the signal energy.

In order to further improve the noise utilization rate and enhance the detection of weak signals, some scholars have proposed some improved resonance models [22–25]. In the literature [23,24], the Woods-Saxon monostable model and the power function type single potential model are respectively combined with the Gaussian Potential (GP) model to form two special bistable systems, and the simulations prove that they are better than the classical bistable system. The literature [25] combines the bistable system and the GP model to form a special tristable system, and proves that it is better than the bistable system. The above research analyses show that the effects of highlighting signal characteristics and attenuating noise are obtained by improving and optimizing the monostable and bistable model. Since the GP model is a special single potential well structure, it is combined with the monostable and bistable models to form the special bistable and tristable systems with better performance. As mentioned above, the performance of the classical tristable system is better than the traditional monostable and bistable systems. If the advantages of the GP model and the tristable system are fully utilized to construct a class of composite multi-stable model, it is expected to obtain the SR model with better performance, however there are no relevant research results reported so far.

With the diversification of potential models of SR, different models have one or more parameters. In order to obtain the best detection effect, it is essential to optimize the parameters of the SR system. For the novel composite multi-stable system, more structural parameters need to be optimized, therefore it is necessary to further study the parameter-induced adaptive SR. At present, the scholars mainly use particle swarm optimization algorithm [19,26], artificial fish swarm algorithm [25], genetic algorithm [27], fruit fly algorithm [28] and other group intelligent optimization algorithms to realize multi-parameter optimization of the SR system. What's more, they have achieved good results. Different from other intelligent optimization algorithms, the individual-person of brain storm optimization (BSO) algorithm not only has the subconscious cooperation and interaction abilities of other animals, but also has strong logical reasoning and thinking innovation abilities [29]. BSO algorithm learns from the class center, so it is more likely to jump out of the local optimum than other group intelligent optimization algorithms.

The rest of this paper is arranged as follows. In Section 2, the composite multi-stable potential model is proposed. Section 3 shows the SR system driven by the composite multi-stable potential model, and introduces the implementation process of parameter-induced adaptive SR based on the differential brain storm optimization (DBSO) algorithm. In Section 4, the output response performances of composite multi-stable SR system are analyzed under Gaussian white noise and α stable noise, and it is compared with the SR systems based on the traditional tristable model and composite tristable model constructed by the bistable and GP models. Besides, the adaptive detection of the multiple high-frequency weak signal is realized. Finally, the conclusions are drawn in Section 5.

2. Potential model

2.1. Tristable potential model

A class of nonlinear tristable potential function is shown in Eq. (1).

$$U_1(x) = \frac{a}{2}x^2 - \frac{1+a}{4b}x^4 + \frac{1}{6c}x^6 \tag{1}$$

where a, b, c are the system parameters, a and c are positive real numbers, and b is a non-zero real number. The shape of the tristable potential function is shown in Fig. 1.

As can be seen from Fig. 1, the potential function has three minimum points (steady-state points) and two maximum points, as shown in Eqs. (2) and (3) respectively.

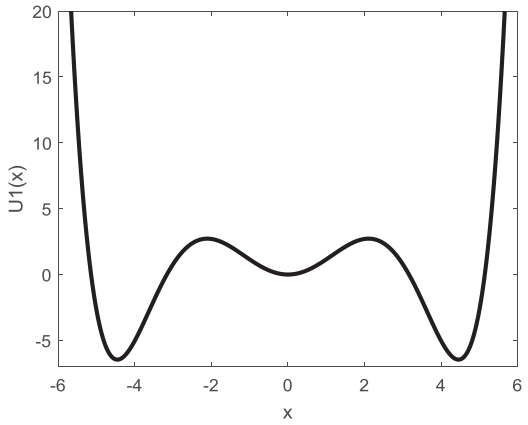

Fig. 1. Tristable potential function.

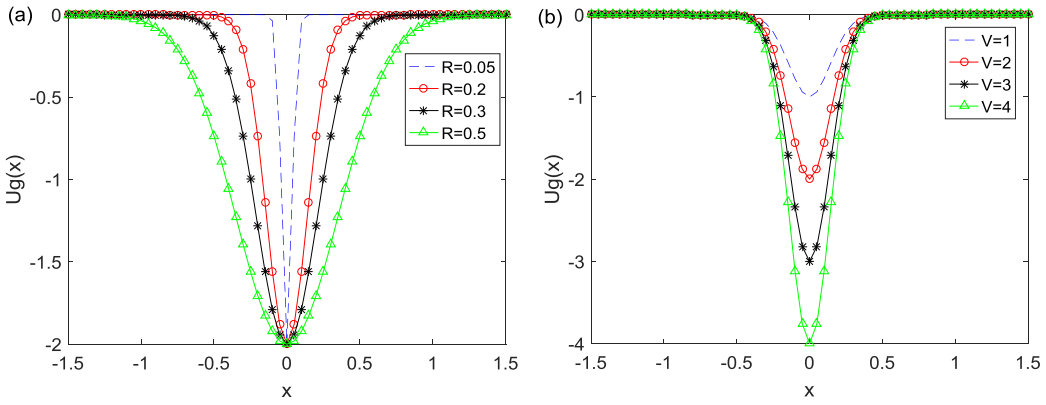

Fig. 2. (a) The potential function under different R at $V = 2$; (b) The potential function under different V at $R = 0.2$.

$$x_{\min} = 0, \pm\sqrt{\frac{c}{2}\left(\frac{1+a}{b} + \sqrt{\left(\frac{1+a}{b}\right)^2 - \frac{4a}{c}}\right)} \tag{2}$$

$$x_{\max} = \pm\sqrt{\frac{c}{2}\left(\frac{1+a}{b} - \sqrt{\left(\frac{1+a}{b}\right)^2 - \frac{4a}{c}}\right)} \tag{3}$$

2.2. Gaussian potential (GP) model

In nuclear physics, GP model is commonly used to describe the nuclear scattering. It has been found that the GP model has a beneficial effect in solving differential equations, especially Schrodinger equation [23]. The Fokker–Planck equation (FPE) is commonly used to study the motion problem of Brownian particles in SR, and FPE can be transformed into FP-Schrodinger equation. Therefore, the introduction of the GP model is of great significance for the studies of SR. The radial GP model can be expressed as Eq. (4).

$$U_g(x) = -V\exp\left(-\frac{x^2}{R^2}\right) \tag{4}$$

In Eq. (4), V represents the depth of the potential well, and R indicates the width of the potential well. Fig. 2 shows the effect of different parameters on the shape of the GP model. It can be seen that the two ends of the potential well converge rapidly to zero, which can be regarded as a special single potential well structure. In Fig. 2(a), with the decrease of R, the width of the potential well decreases gradually and the wall of the potential well gradually becomes steep, but its depth remains unchanged. It can be seen from Fig. 2(b) that the depth of the potential well is uniquely characterized by V. Consequently, there is no coupling between the parameters of the GP model, and the parameters V and R determine the depth and width of the potential well respectively.

2.3. Composite multi-stable potential model

The above tristable potential model and GP model are combined to construct a novel composite multi-stable potential model, whose potential function is shown in Eq. (5).

$$U(x) = U_1(x) - U_g(x) = \frac{a}{2}x^2 - \frac{1+a}{4b}x^4 + \frac{1}{6c}x^6 + V\exp\left(-\frac{x^2}{R^2}\right) \tag{5}$$

For the given parameters $a = 2.65$, $c = 33.3$, $R = 1$, the potential function shapes of composite multi-stable system under different conditions are shown in Fig. 3.

It can be seen from Fig. 3 that the potential model can be switched between monostable, bistable and multi-stable models under the action of different parameters. Therefore, the system parameters can be adjusted according to the characteristics of different input signals to realize the switching between different steady-state models. It makes the input signal and the resonance model match optimally to achieve the best detection of unknown weak signals. In Fig. 3(a) and (b), the depth of the intermediate potential well of the original tristable model becomes smaller at $V = 1$ due to the introduction of the GP model. But when the value of V becomes larger, that is, V is equal to 2, 2.5, and 3, the original three steady-state becomes four steady-state. Meanwhile, it can be seen that the function value of $U(x)$ is always equal to the value of the parameter V at $x = 0$.

This model makes full use of the advantages of the tristable potential model and the GP model. When the Brownian particles do not have enough energy to jump across the barriers between the middle and the two sides of the potential wells in the tristable system, they can only reciprocate in the middle potential well, and the noise energy cannot be converted into the signal energy

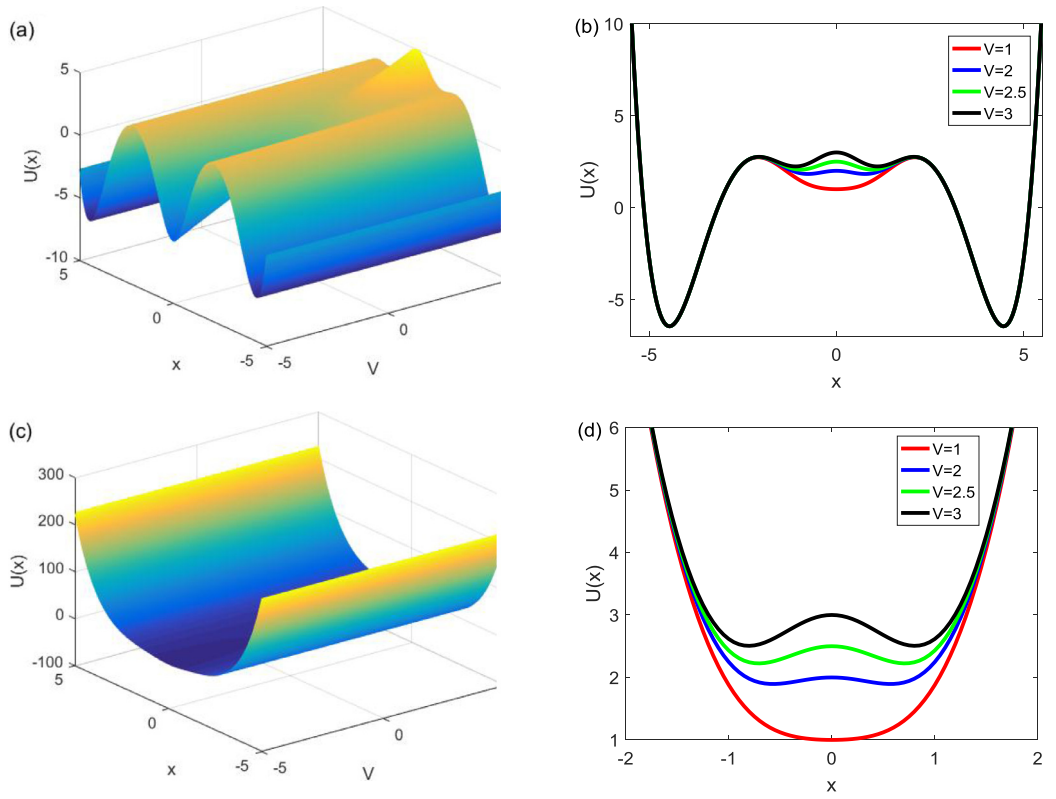

Fig. 3. (a)$U(x)$ under different V at $b = 5$; (b) the curves of $U(x)$ when V is equal to 1, 2, 2.5, 3 respectively at $b = 5$; (c)$U(x)$ under different V at $b = -5$; (d) the curves of $U(x)$ when V is equal to 1, 2, 2.5, 3 respectively at $b = -5$.

sufficiently. At this time, the GP model acts as a potential obstacle, which can buffer the movement of the particles between the potential wells. In other words, it can make the particles realize the periodic reciprocating movement by means of step-by-step multi-stage transitions. Meanwhile, because the particles need to jump over multiple barriers, the noise energy can be weakened to a certain extent and it can be transferred to the useful signal to the maximum extent. It can realize the detection of the weak signals with extremely low SNR, and improve the weak signal processing capability of SR system.

3. SR system

3.1. Composite multi-stable SR system

Under the joint action of external force and noise, the overdamped motion of the Brownian particles in the composite multi-stable system can be described by the Langevin equation, as shown in Eq. (6).

$$\frac{dx}{dt} = -U'(x) + s(t) + \eta(t) \tag{6}$$

where $x(t)$ is the output of the SR system, $U(x)$ is the potential function of the system, $s(t)$is the input signal, and $\eta(t)$ is the additive noise. In this paper, $s(t)$is shown in Eq. (7).

$$s(t) = \sum_{i=1}^{n} A_i \sin(2\pi f_i t) \tag{7}$$

where A_i is the amplitude of the ith signal, f_i is the frequency of the ith signal, and n represents the number of input signals.

In this paper, SR phenomena of the composite multi-stable system under Gaussian white noise and αstable noise environments are studied respectively. In Eq. (6), $\eta(t) = \sqrt{2D}\,\xi(t)$, $< \eta(t)\eta(t+\tau) > = 2D\delta(t)$, where D represents the noise intensity, $\xi(t)$ is the Gaussian white noise with the mean of 0 and the variance of 1 and α stable noise respectively. α stable noise is generated by Janicki–Weron algorithm [8,30]. Substituting Eq. (5) into Eq. (6) can obtain Eq. (8) .

$$\frac{dx}{dt} = -ax + \frac{1+a}{b}x^3 - \frac{1}{c}x^5 + \frac{2Vx}{R^2}\exp\left(-\frac{x^2}{R^2}\right) + s(t) + \eta(t) \tag{8}$$

In this paper, the fourth-order Runge–Kutta algorithm [17] is used to solve Eq. (8). α stable noise has the significant pulse

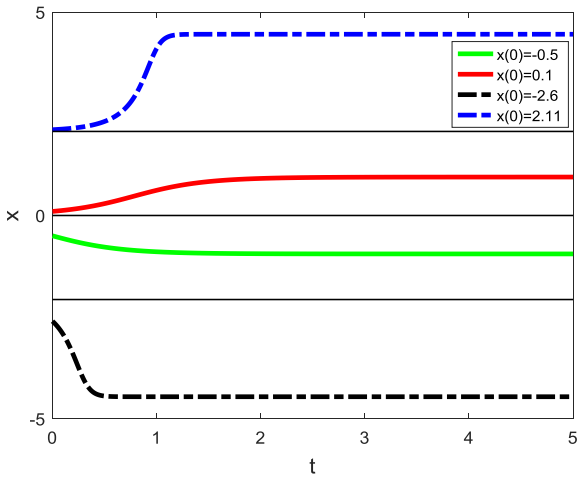

Fig. 4. Time histories of Eq. (8) in different initial states without periodic force and noise.

characteristics, which causes the paths of the particles to change rapidly and even infinitely during the long jump process. Therefore, in the numerical simulation, the output signal needs to be truncated artificially [31,32] to solve the problem that the hopping trajectories of the particles are large infinitely. The truncation measure adopted in this paper is that when $|x(t)| > 5$, let $x(t) = sign(x(t)) \times 5$. In the absence of periodic force and noise, the motion curves of the particles in the composite multi-stable potential well under different initial states are shown in Fig. 4, where the system parameters are $a = 2.65$, $b = 5$, $c = 33.3$, $V = 2.5$, $R = 1$. It can be seen that the particles move gradually from the unsteady points to the steady points, and finally stabilize at the steady points.

3.2. Measurement index

The SR effect of the single-frequency signal can be measured by the signal-to-noise ratio (SNR), and the expression is shown in Eq. (9).

$$SNR = 10\lg\frac{S(\omega)}{N(\omega)} = 10\lg\frac{S(\omega)}{P - S(\omega)} \tag{9}$$

where ω is the signal frequency, $S(\omega)$ is the signal power, $N(\omega)$ is the noise power, and P is the total power of the system. The output SNR reflects the ability of SR system to filter and purify useful signals.

In order to measure the overall detection effect of the SR system on the multi-frequency signal, the mean SNR (MSNR) is used as a metric, and the definition is shown in Eq. (10).

$$MSNR = \frac{\sum_{i=1}^{n} SNR_i}{n} \tag{10}$$

where SNR_i is the SNR of the ith signal to be measured.

3.3. Parameter-induced adaptive SR

In order to realize the fast enhancement detection of weak signals, the differential brain storm optimization (DBSO) algorithm [29] is used to optimize multiple parameters collaboratively in the SR system. The brain storm optimization (BSO) algorithm is a method based on stimulating thinking to produce or create new ideas. It abstracts the optimization process into two processes: 'gathering' and 'dispersing'. After initializing the population, the population is classified by clustering, and the individuals are updated by various interactions of intra-class, inter-class and class center to complete the 'gathering' operation. On this basis, a certain range of 'dispersing' is achieved by variation operation to enhance the diversity of the population.

In the BSO algorithm, the variation is to diverge thinking, gather ideas and generate new information based on the new individuals generated by clustering center so as to obtain more new individuals. The standard BSO algorithm uses Gaussian variation, which produces the essentially fixed variation range, and does not take full advantage of the individual information in the current population. However, differential variation is to use the differences between different individuals in the population to disturb the target individual to achieve individual variation. It is the sharing of the information between individuals, which can be adjusted adaptively according to the degree of individual dispersion within the population. Differential variation can better balance the local and global search in the search process, thereby improving the performance of the algorithm effectively. Therefore, the DBSO algorithm is adopted in this paper. The formula of differential variation is shown in Eq. (11).

Input: N (the population size), E (the individual dimension), T (the maximum number of iterations), M (the number of clusters), P_{5a} (the probability of changing the cluster center), P_{6b} (the probability of selecting a cluster), P_{6biii} (the probability of selecting the cluster center while selecting a cluster), P_{6c} (the probability of selecting the cluster center while selecting two clusters).

Output: P (final population);

1: P ←Initialize population; /* Generate N individuals randomly and evaluate N individuals. */

2: **while** the maximum number of iterations is not reached **do**

3: Cluster; /* Cluster N individuals into M classes by K-means clustering algorithm. */

4: **if** $rand < P_{5a}$ **then**

5: Generate an individual randomly to replace any one of the cluster centers;

6: **end if**

7: $P_{selected}$ ←The process of brainstorming is carried out to gain the selected individuals;

8: New individuals are generated by mutation according to Eq. (11);

9: P ←Update population;

10:**end while**

Fig. 5. The pseudo code of DBSO algorithm.

$$x_{new}^{d} = \begin{cases} rand(L_d, H_d) \ \ if \ \ rand() < P_r \\ x_{selected}^{d} + rand(0, 1) \times (x_1 - x_2) \ \ else \end{cases} \tag{11}$$

where $x_{selectd}^{d}$ is the dth dimension of the selected individual, x_{new}^{d} is the dth dimension of the generated individual. L_d and H_d are the lower and upper bounds of the dth dimension individual. x_1 and x_2 are the two different individuals selected in the contemporary global field. In order to maintain the diversity of the population and prevent it from falling into local optimum, the open probability P_r is set, generally taking the empirical value as $P_r = 0.05$. The pseudo code of DBSO algorithm is shown in Fig. 5.

In Fig. 5, P_{5a}, P_{6b}, P_{6biii}, P_{6c} are the given values between 0 and 1, which are used to describe the presupposed selection probability. According to the four different probability values, the generation mode of new individuals is selected to simulate the chatting process in the brainstorming process. On this basis, random values are added to enhance the diversity of the population by mutation to simulate the arrangement and adjustment of the scheme. The specific operation is shown in the literature [29].

For the fast enhancement detection of single-frequency and multi-frequency signals, the output SNR and MSNR are selected as the fitness function respectively. The fitness function adopted here is the objective optimization function. The DBSO algorithm is used to collaboratively optimize the structural parameters *a, b, c, V, R* of the composite multi-stable SR system. The parameters of the system are searched when the SNR reaches the maximum, so that the SR system can achieve the optimal effect and the adaptive detection of weak signal can be realized. The flow chart of the algorithm is shown in Fig. 6.

4. Simulations and analyses

4.1. Influences of system parameters V and R on SR effect

The driving signal is $s(t) = A\sin(2\pi ft)$, where $A = 0.1$, $f = 0.01Hz$. The number of sampling points is $N = 4096$ and the sampling frequency is $f_s = 4.08Hz$. When the background noise is Gaussian white noise, the noise intensity is $D = 1.5$. And when the background noise is α stable noise, where $\alpha = 1.5$, $\beta = 0$, $\sigma = 1$, $\mu = 0$, the noise intensity is $D = 0.31$. Fixing the system parameters *a, b, c* as $a = 2.65$, $b = 5$, $c = 33.3$, the variation curves of the output SNR with V and R under two different noise environments are shown in Figs. 7 and 8. The results in Figs. 7 and 8 are the average values of 20 groups of experiments, the red curves are the smooth fitting curve (via polynomial fitting method) of the original curves (black curves).

It can be seen from Figs. 7(a) and 8(a) that with the gradual increase of V at $R = 1$, the variation trends of SNR with V are basically

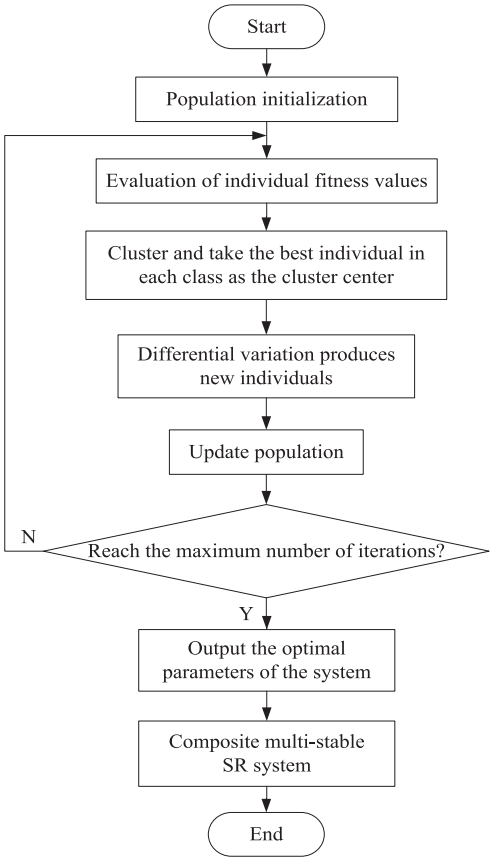

Fig. 6. Flow chart of adaptive composite multi-stable SR based on DBSO.

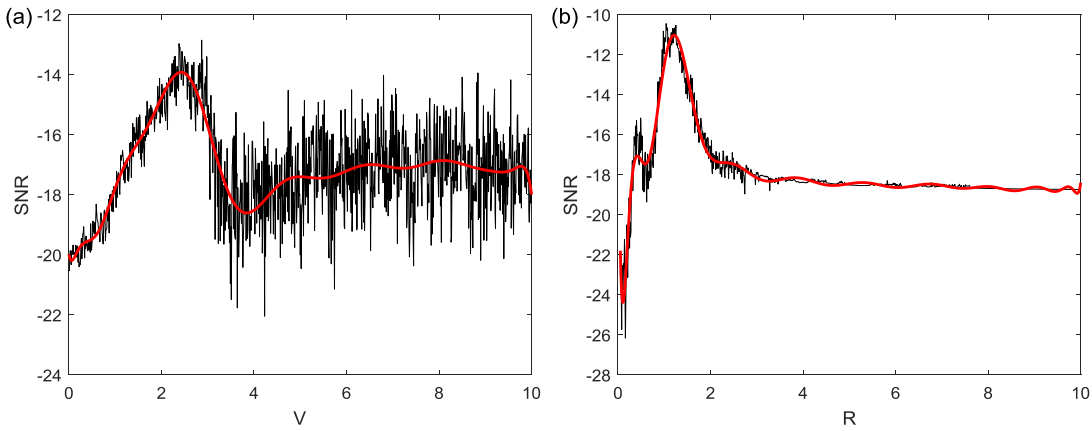

Fig. 7. The curves of SNR with V and R under Gaussian white noise environment: (a) the curve of SNR with V at $R = 1$; (b) the curve of SNR with R at $V = 2.5$.

the same in both noise environments, and the overall trends appear to increase first and then decrease. When the values of V are in the interval [2, 4], SNR reaches a peak. It can be seen from Figs. 7(b) and 8(b) that there is a nonlinear relationship between SNR and R, and the overall trends also appear to increase first and then decrease. The difference is that when $R > 3$, the values of SNR do not fluctuate greatly under Gaussian white noise environment and are basically stable near a certain value, while the values of SNR always fluctuate within a small range of the mean under α stable noise environment. In addition, it can be seen that SNR is more sensitive to the change of the system parameter V, and the slight change of V will affect the system output to a large extent, so it is very important to select the parameters of SR system. The above results indicate that when the parameters a, b, c in the composite multi-stable system are determined, the output SNR of the SR system can be improved under the auxiliary action of the parameters V and R. It is more flexible and maneuverable and easier to match the best resonance model according to the characteristics of the input

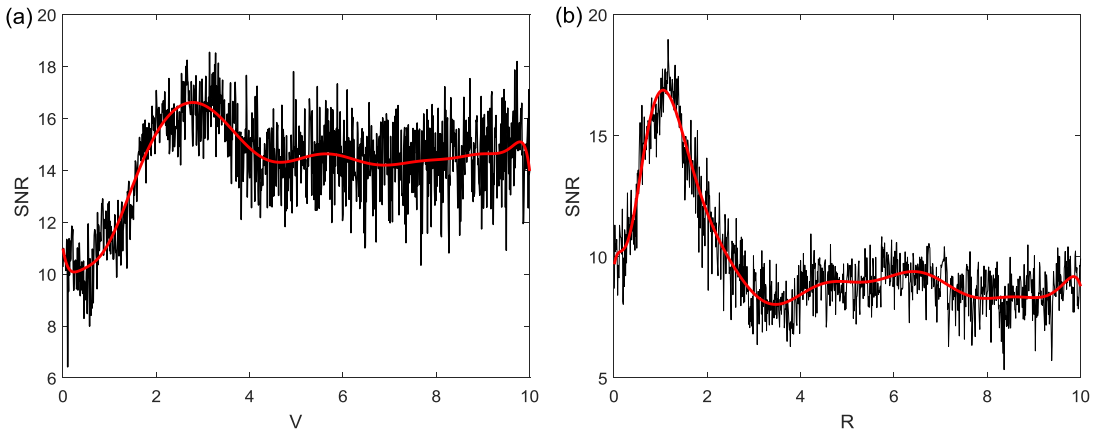

Fig. 8. The curves of SNR with V and R under α stable noise environment: (a) the curve of SNR with V at $R = 1$ (b) the curve of SNR with R at $V = 2.5$.

signal, which has stronger weak signal processing capability.

4.2. Performance analyses of composite multi-stable SR system

Set the amplitude and frequency of the single-frequency signal as $A = 0.1$ and $f = 0.01$Hz. The number of sampling points is $N = 4096$, the sampling frequency is $f_s = 4.08$Hz, and the background noise is Gaussian white noise and α stable noise of $\alpha = 1.5$, $\beta = 0$, $\sigma = 1$, $\mu = 0$. Fig. 9 shows the variation curves of the output SNR with the noise intensity D under two different noise environments, and the results are the average values of 20 groups of experiments. In Fig. 9, the parameters of the composite multi-stable SR system are $(a, b, c, V, R) = (2.65, 5, 33.3, 2, 1)$, and the parameters *a, b, c* in the tristable system are consistent with that in the composite multi-stable system. Since α stable noise itself has significant impact characteristics, the noise intensity intervals of Gaussian white noise and α stable noise in Fig. 9 are set to [0,4] and [0,1] respectively. It can be seen from Fig. 9 that the output SNR of the composite multi-stable system is higher than the traditional tristable system as a whole in both noise environments. This is because the potential model of the composite multi-stable system, noise and input signal achieve good synergy, improving the noise utilization rate. The above analyses show that the composite multi-stable SR system can ameliorate the detection effect of weak signals on the basis of the tristable SR system.

Similarly, the amplitude and frequency of the signal is taken as $A = 0.1$ and $f = 0.01$Hz. The number of sampling points is $N = 4096$ and the sampling frequency is $f_s = 4.08$Hz. The detection results of the tristable and composite multi-stable SR systems under the Gaussian white noise of $D = 1.5$ are shown in Fig. 10.

Fig. 10(a) shows the time domain diagram of the signal submerged in Gaussian white noise, which is equivalent to the noisy signal collected in practice. The power spectrum diagram of the noisy signal after fast Fourier transform (FFT) is shown in Fig. 10(b). It can be seen that the useful information of the signal cannot be observed directly from the time domain and the frequency domain diagrams. At this time, the input SNR is -28.44 dB. In Fig. 10(c), it can be seen from the time-domain diagram that the amplitude of the output signal of the system is limited between the maximum points of the tristable system. This is because the noise energy is small enough to cause the particle to transit between the potential wells. It can only oscillate back and forth in the middle potential

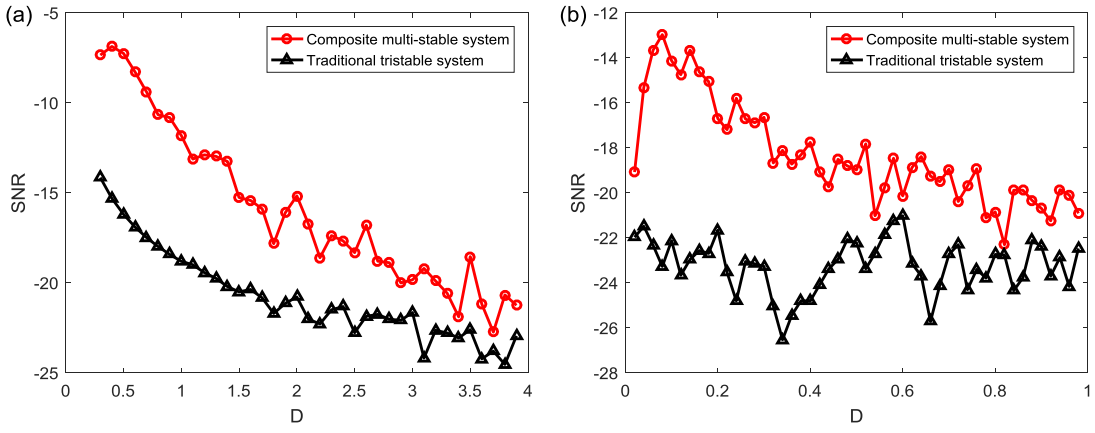

Fig. 9. (a) The curves of SNR with D under Gaussian white noise environment; (b) the curves of SNR with D under α stable noise environment.

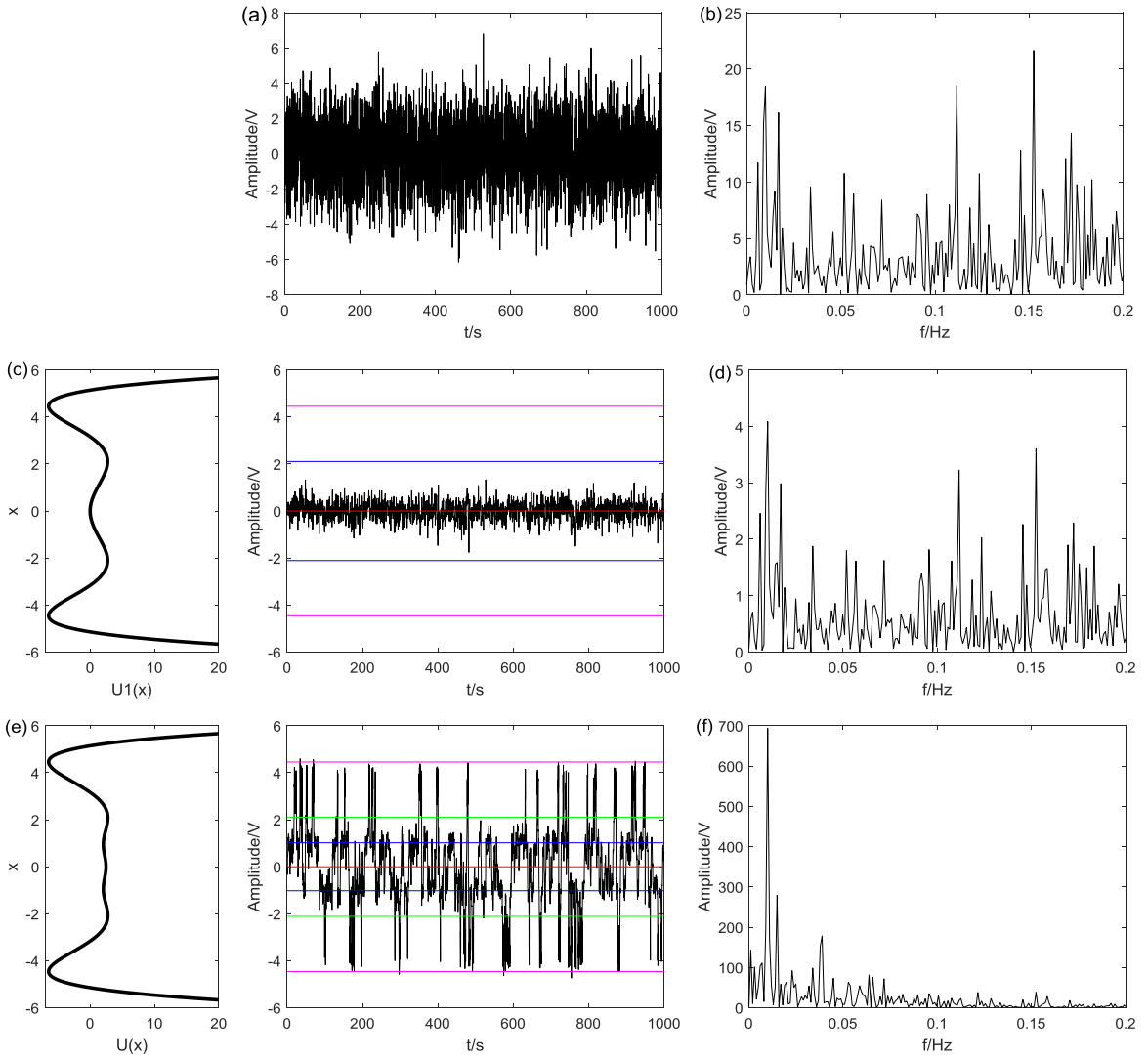

Fig. 10. The detection results under Gaussian white noise environment: (a) the time domain diagram of the noisy signal; (b) the power spectrum diagram of the noisy signal; (c) the tristable model when $a = 2.65$, $b = 5$, $c = 33.3$ and the time domain diagram of its resonance output signal; (d) the output power spectrum diagram of the tristable SR system; (e) the composite multi-stable model when $a = 2.65$, $b = 5$, $c = 33.3$, $V = 2.47$, $R = 1$ and the time domain diagram of its resonance output s;ignal; (f) the output power spectrum diagram of the composite multi-stable SR system.

well of the tristable system. The periodic characteristics of the signal cannot be highlighted and be identified effectively in the corresponding spectrum diagram, that is, Fig. 10(d). It can be seen from Fig. 10(e) that the particle can transit between potential wells in the composite multi-stable system, and the periodicity of the output signal is significant. An obvious sharp peak can be seen at the frequency of 0.01 Hz in Fig. 10(f) and the weak signal can be detected visually. The composite multi-stable system has larger output SNR (-8.59 dB) than the tristable system (-18.23 dB). This is because the local shape of the tristable potential well is changed under the action of GP model, and the effective barrier height is reduced. Therefore a good match between the nonlinear system, the noise and the useful signal is achieved. The noise utilization rate is improved, and the weak periodic signal is enhanced and detected.

Under α stable noise environment of $D = 0.31$, where $\alpha = 1.5$, $\beta = 0$, $\sigma = 1$, $\mu = 0$, the input SNR is -33.33 dB, and the detection results of the tristable and composite multi-stable SR systems are shown in Fig. 11. It can be seen from Fig. 11(a) that α stable noise has significant peak and pulse characteristics compared with Gaussian white noise. The time domain characteristics of the periodic signal are not seen at all under α stable noise environment, and its frequency domain information also cannot be recognized. It can be seen from Fig. 11(c) and (d) that the original tristable SR system highlights the frequency domain characteristics of the signal to a certain extent, but it cannot detect the weak signal effectively, and the output SNR is -20.18 dB. Meanwhile, on the basis of the fixed system parameters *a, b, c*, the weak signal can be detected effectively only by changing the parameters V and R in the composite multi-stable system. The output SNR is -11.15 dB, which is 9.03 dB higher than the tristable system. As a result, compared with the tristable SR system, the composite multi-stable SR system is easier to match the optimal resonance model to maximize the useful signal energy and improve the detection effect of weak signals. In addition, the consistent conclusion is drawn under the two most

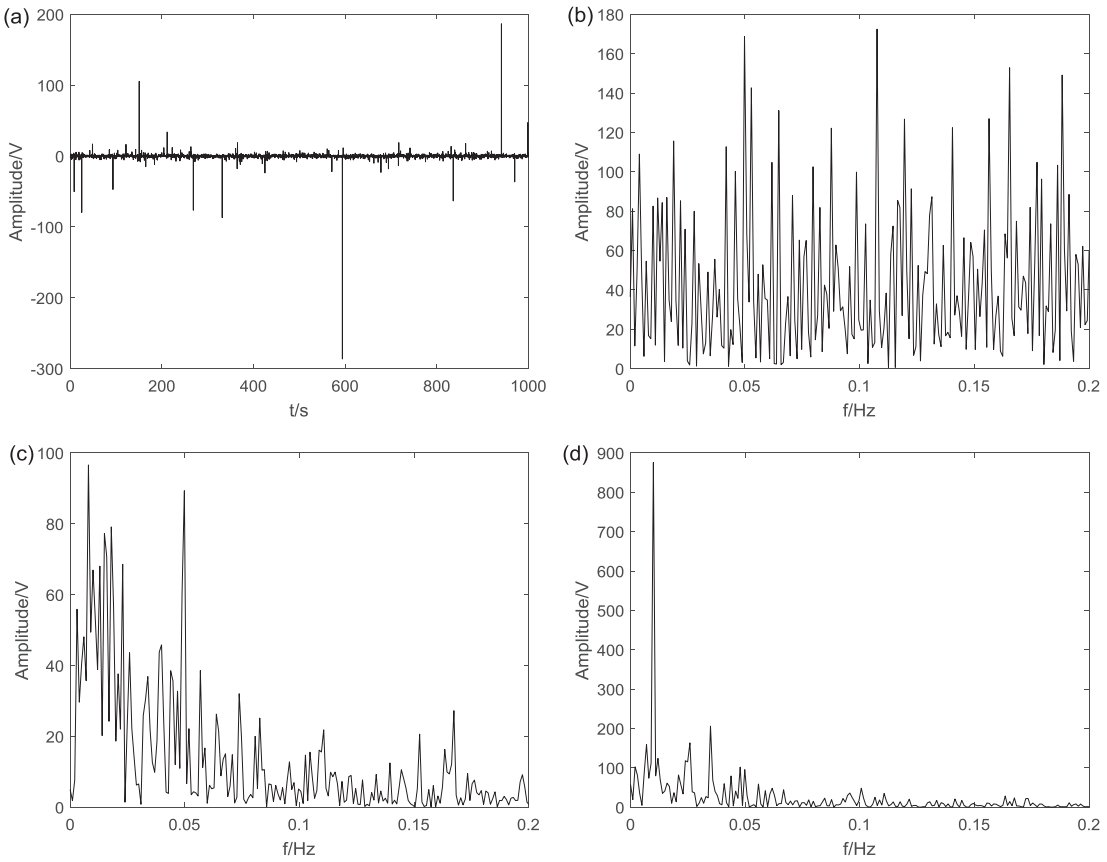

Fig. 11. The detection results under α stable noise environment: (a) the time domain diagram of the noisy signal; (b) the power spectrum diagram of the noisy signal; (c) the output power spectrum diagram of tristable SR system when $a = 2.65$, $b = 5$, $c = 33.3$; (d) the output power spectrum diagram of composite multi-stable SR system when $a = 2.65$, $b = 5$, $c = 33.3$, $V = 2.51$, $R = 1$.

Table 1
Parameters setting of the DBSO algorithm.

N	T	M	P_{5a}	P_{6b}	P_{6biii}	P_{6c}
100	200	5	0.1	0.5	0.4	0.5

Table 2
Comparisons of the SNRs for different systems.

System type	Signal amplitude	Input SNR	Optimized system parameters					Output SNR
			a	b	c	V	R	
Composite multi-stable system	0.01	−30.89	0.92	−7.57	94.03	1.50	0.37	−5.12
Traditional tristable system			0.50	4.59	100			−5.20
Composite tristable system			7.93	0.79		1.24	10	−7.00
Composite multi-stable system	0.001	−29.89	2.95	5.14	28.21	8.37	2.70	−5.73
Traditional tristable system			0.93	4.02	47.42			−5.34
Composite tristable system			8.23	0.67		4.84	6.79	−6.75
Composite multi-stable system	0.0001	−29.80	1.20	3.58	30.56	1.87	2.92	−4.33
Traditional tristable system			1.64	2.40	10			−6.12
Composite tristable system			7.90	1.46		3.30	8.95	−5.89

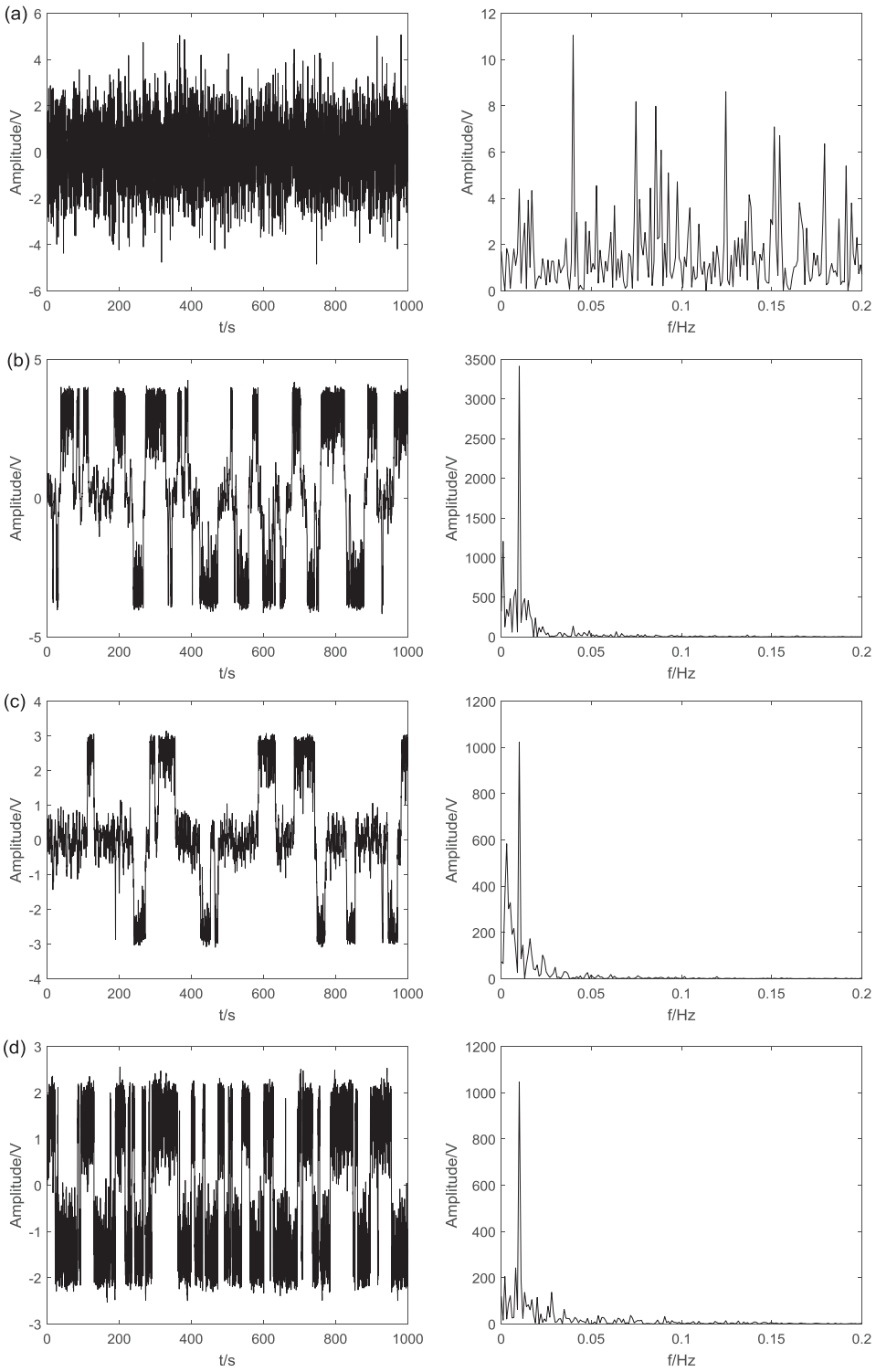

Fig. 12. The detection results of three kinds of systems when the signal amplitude is 0.0001: (a) the time domain and power spectrum diagrams of the input noisy signal; (b) the output time domain and power spectrum diagrams of the composite multi-stable system; (c) the output time domain and power spectrum diagrams of the traditional tristable system; (d) the output time domain and power spectrum diagrams of the composite tristable system.

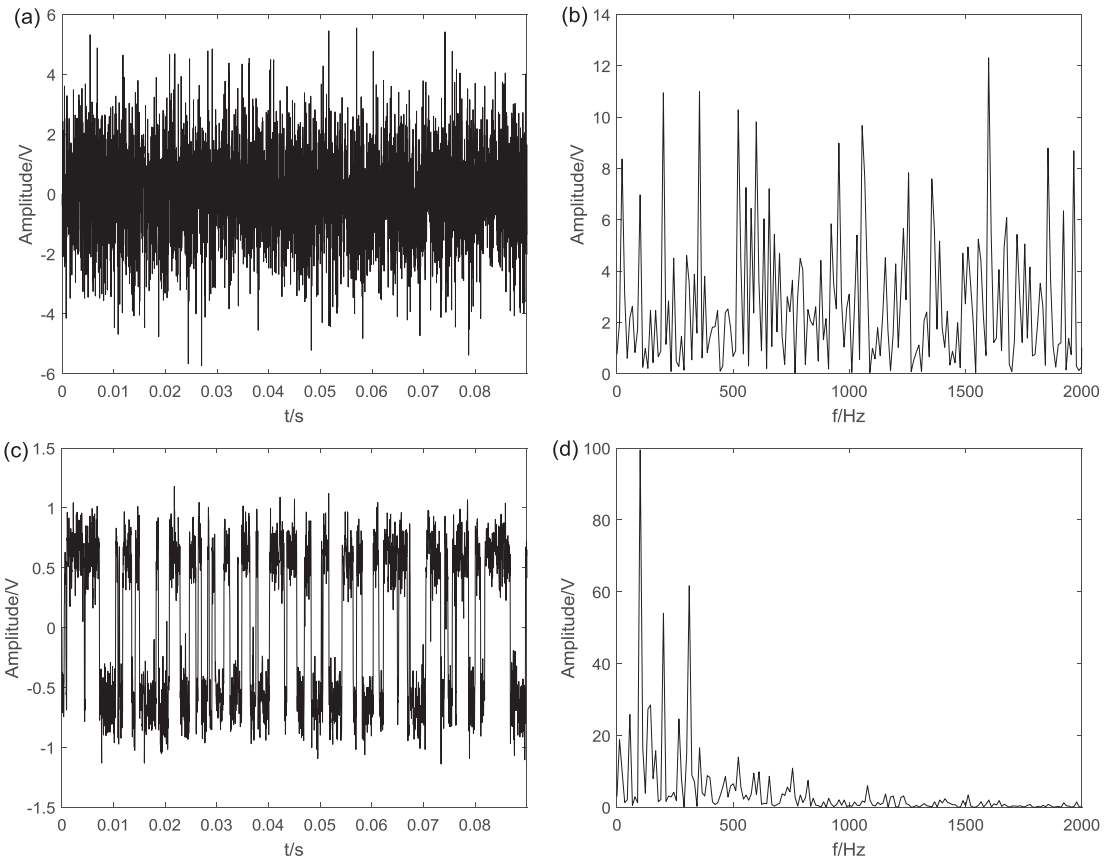

Fig. 13. The detection results of the multiple high-frequency signal in Gaussian white noise environment: (a) the time domain diagram of the noisy signal; (b) the power spectrum diagram of the noisy signal; (c) the output time domain diagram of SR system; (d) the output power spectrum diagram of SR system.

representative noise environments of Gaussian white noise and α stable noise.

4.3. Comparisons with other potential models

Weak signals can be understood from two aspects: one is that the amplitude of the useful signal is very weak relative to noise or interference, which is the relative meaning of the weak signal. And the other is that the amplitude of the useful signal is extremely small, such as detecting voltage signals of the magnitude of uV, nV and pV, which is the absolute meaning of the weak signal. Most scholars detect weak signal submerged in strong noise background, but they often neglect the case where the amplitude of the useful signal is extremely small. In the case where the amplitude of the signal itself is extremely small, taking the detection in Gaussian white noise environment as an example, the noise intensity is set to $D = 1$ and the frequency of the signal is $f = 0.01$. The DBSO algorithm is used to optimize the parameters of composite multi-stable system, traditional tristable system and the composite tristable system constructed by bistable and GP models [25] respectively. The parameters of DBSO algorithm are set as shown in Table 1. And the detection results of three kinds of systems for different levels of weak signals are shown in Table 2.

It can be seen from Table 2 that when the signal amplitude is 0.01 and 0.001, the output SNRs of the composite multi-stable system are approximate to the tristable system, while the output SNRs of the composite tristable system are relatively smaller than that of them. When the signal amplitude is smaller, that is 0.0001, the output SNR of the composite multi-stable system is larger than that of the traditional tristable system and the composite tristable system. Fig. 12 shows the detection results of the three kinds of systems when the signal amplitude is 0.0001.

It can be seen from the time domain diagrams in Fig. 12(b)–(d) that the output signal has a significant periodicity. Compared with Fig. 4, it is found that under the joint action of noise and periodic signal, the motion trajectories of particles can be changed, so that the movement of particles can be switched between potential wells according to the modulation frequency of the signal. The switching speed makes the output signal synchronize with the input weak periodic signal, thus the periodic signal component of the system output can be enhanced. As can be seen from the power spectrum diagrams in Fig. 12(b)–(d), the spectrum amplitudes of the output signal of the traditional tristable system and the composite tristable system are about 1000, while that of the composite multi-stable system is close to 3500. It further highlights the useful signal, which is conducive to the enhancement and extraction of the

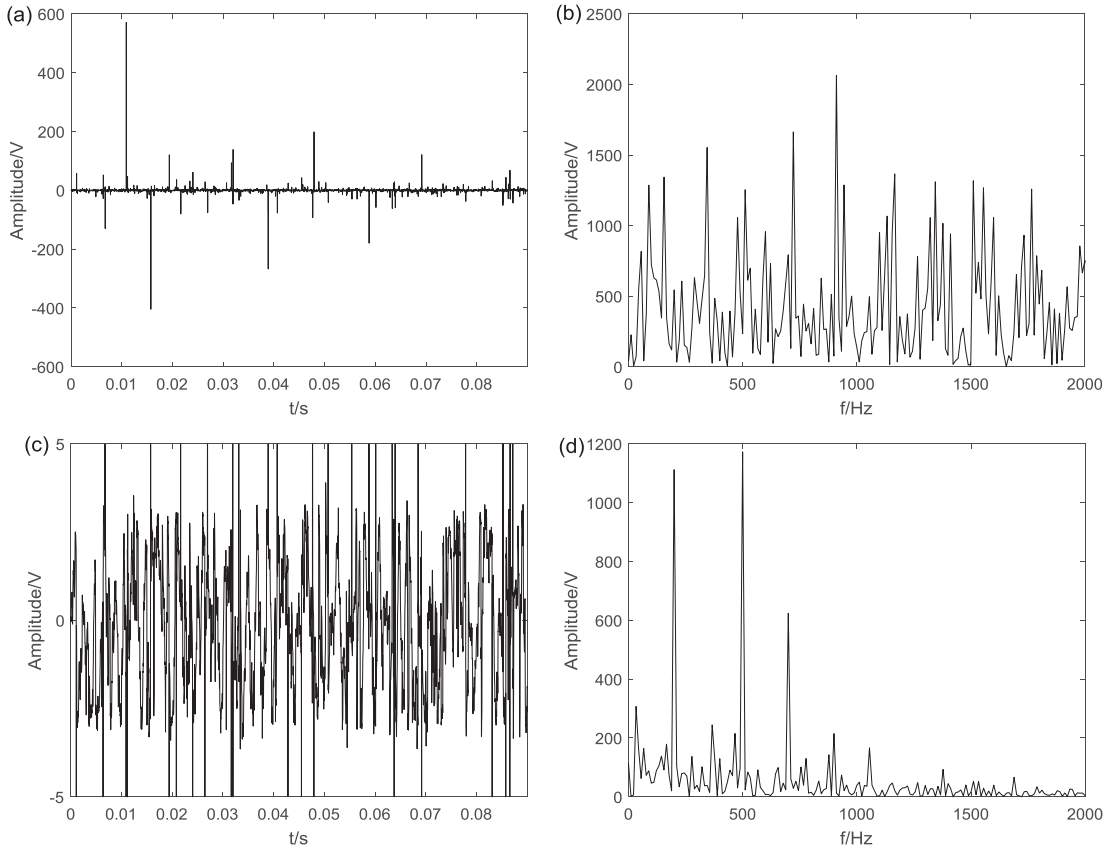

Fig. 14. The detection results of the multiple high-frequency signal in α stable noise environment: (a) the time domain diagram of the noisy signal; (b) the power spectrum diagram of the noisy signal; (c) the output time domain diagram of SR system; (d) the output power spectrum diagram of SR system.

weak characteristic signals, and lays the foundation for detecting the extremely weak fault characteristic signals in the engineering applications.

4.4. The detection of the multiple high-frequency weak signal

The traditional SR is limited by the adiabatic approximation theory and the linear response theory, which is only suitable for dealing with small parameter signals. In practical engineering, large parameter signals are often encountered. For example, the frequencies of the fault characteristic signal may be more than one, and generally in dozen of Hz, hundreds of Hz, or even thousands of Hz in fault diagnosis. For the detection of high-frequency signals, the parameter compensation SR is an effective method [30]. Consequently, the adaptive SR combined with the parameter compensation method is adopted to deal with the detection problem of the multiple high-frequency weak signal.

The parameters of the DBSO algorithm are set as shown in Table 1. The ranges of system parameters are $a \in [0, 10]$, $b \in [-10, 10]$, $c \in [0, 100]$, $V \in [0, 10]$, $R \in [0, 10]$. The multi-frequency signal is $s(t) = A_1 \sin(2\pi f_1 t) + A_2 \sin(2\pi f_2 t) + A_3 \sin(2\pi f_3 t)$, in which the amplitudes of the signal are $A_1 = A_2 = A_3 = 0.1$, and the frequencies are $f_1 = 100$Hz, $f_2 = 200$Hz, $f_3 = 300$Hz respectively. In Gaussian white noise environment, the noise intensity is $D = 1.2$. The number of sampling points is $N = 4096$, and the sampling frequency is $f_s = 45.5$KHz. Taking the output MSNR as the fitness function, the parameter compensation SR method is used, and the compensation parameter is $K = 10000$. The input MSNR of the system is -28.47 dB. The five parameters of the composite multi-stable SR system are optimized collaboratively by the DBSO algorithm, and the optimized parameters are $(a, b, c, V, R) = (0.02, -0.52, 52.31, 0.90, 0.36)$. Under this set of parameters, the detection results for the multiple high-frequency weak signal are shown in Fig. 13.

It can be seen from Fig. 13(a) and (b) that the signal is submerged completely in Gaussian white noise, and the useful information of the signal cannot be observed directly from the time domain and the frequency domain diagrams. When the noisy signal is sent into the composite multi-stable SR system, the time domain diagram of the output signal shown in Fig. 13(c) can be obtained. It can be observed from Fig. 13(c) that the amplitude of the signal is amplified. This is because when SR occurs, the particles need to overcome the barriers to move in the multi-stable system, and the potential difference between the wells of the composite multi-stable system is much larger than the amplitude of the useful signal. The output frequency domain diagram of the system is shown in Fig. 13(d) and it can be observed clearly that three peaks appear at the frequencies of 100 Hz, 200 Hz, and 300 Hz. These three peaks are just the

frequencies of the signal to be detected. The output MSNR of the system is −11.92 dB, and the SNR is increased by 16.55 dB.

In α stable noise environment, where $\alpha = 1.2$, $\beta = 0$, $\sigma = 1$, $\mu = 0$, the noise intensity is $D = 0.31$. The amplitudes of the multi-frequency signal are $A_1 = A_2 = A_3 = 0.1$, and the frequencies are $f_1 = 200$Hz, $f_2 = 500$Hz, $f_3 = 700$Hz respectively. The number of sampling points is $N = 4096$, and the sampling frequency is $f_s = 45.5$KHz. Adaptive SR based on DBSO is used to detect multiple high-frequency weak signal. The optimized system parameters are $(a, b, c, V, R) = (0.60, 9.94, 58.47, 1.62, 4.96)$, and the detection results are shown in Fig. 14.

It can be seen from Fig. 14(a) and (b) that the signal is submerged in α stable noise, which cannot be identified from the time domain and the frequency domain diagrams of the noisy signal, and the input MSNR of the system is −32.50 dB. The time domain diagram after the composite multi-stable SR system is shown in Fig. 14(c). Since α stable noise has significant spike characteristics, which causes the path of the particle to change rapidly and even infinitely in the long-time jumping process, so there are some large spikes in the output time domain diagram of the system. The output frequency domain diagram of the system is shown in Fig. 14(d), in which the frequencies of the signal to be detected can be identified effectively. The output MSNR of the system is −10.32 dB and the SNR is improved by 22.18 dB. The simulation results show that this optimization algorithm has good performance, which is effective in dealing with the collaborative optimization of multiple parameters of SR system.

Comparing Figs. 13 and 14, it can be seen that the proposed composite multi-stable SR system can detect the multiple high-frequency signal effectively in two different noise environments. It shows that the system has good immunity to noise types, which is helpful to detect weak signals by applying SR method in different practical environments.

5. Conclusion

In this paper, a novel composite multi-stable potential model is proposed. The output response of SR based on this model is studied. The parameters of SR system are optimized collaboratively by DBSO algorithm to achieve parameter-induced adaptive SR. The SR phenomena driven by Gaussian white noise and α stable noise are studied respectively. The following conclusions are obtained through simulation experiments: 1) Compared with the traditional tristable SR system, the composite multi-stable SR system is easier to match the optimal resonance model and has stronger weak signal processing capability. 2) For different levels of weak signals, the composite multi-stable SR system has better performance than the traditional tristable system and the composite tristable system constructed by the bistable and GP models. 3) The simulation results show that the composite multi-stable SR system has good immunity to noise types, which is conducive to the applications of SR in different fields. These conclusions provide a new adaptive SR method, enriching the research results of SR theory, which have important application value in weak signal detection.

Acknowledgments

This work is supported by the Program of National Natural Science Foundation of China (Grant no. 61871318), the Key Program of National Natural Science Foundation of China (Grant no. 61533014), and the Key Research Program of Shaanxi Provincie (Item no. 2017GY-030).

References

[1] Q.B. He, E.H. Wu, Y.Y. Pan, Multi-scale stochastic resonance spectrogram for fault diagnosis of rolling element bearings, J. Sound Vibr. 420 (2018) 174–184.
[2] Z.X. Wang, Z.J. Qiao, L.G. Zhou, L. Zhang, Array-enhanced logical stochastic resonance subject to colored noise, Chin. J. Phys. 55 (2017) 252–259.
[3] J.M. Li, J.F. Zhang, M. Li, Y.G. Zhang, A novel adaptive stochastic resonance method based on coupled bistable systems and its application in rolling bearing fault diagnosis, Mech. Syst. Signal Process. 114 (2019) 128–145.
[4] Y.C. Hung, C.K. Hu, Constructive role of noise in p53 regulatory network, Comput. Phys. Commun. 182 (2011) 249–250.
[5] L. Zhang, W.B. Zheng, A.G. Song, Adaptive logical stochastic resonance in time-delayed synthetic genetic networks, Chaos: Interdiscip. J. Nonlinear Sci. 28 (4) (2018) 043117.
[6] A. Silchenko, C.K. Hu, Multifractal characterization of stochastic resonance, Phys. Rev. E 63 (2001) 041105.
[7] X. Zhang, Q. Miao, Z.W. Liu, Z.J. He, An adaptive stochastic resonance method based on grey wolf optimizer algorithm and its application to machinery fault diagnosis, ISA Trans. (2017), http://dx.doi.org/10.1016/j.isatra.2017.08.009.
[8] S.B. Jiao, R. Yang, Q. Zhang, G. Xie, Stochastic resonance of asymmetric bistable system with α stable noise, Acta Phys. Sin. 64 (2015) 020502.
[9] G. Zhang, H.W. Li, Wavelet-EMD and stochastic resonance cascade weak signal detection, J. Electron. Meas. Instrum. 32 (2018) 57–65.
[10] Z.J. Qiao, Y.G. Lei, N.P. Li, Applications of stochastic resonance to machinery fault detection: a review and tutorial, Mech. Syst. Signal Process. 122 (2019) 502–536 https://doi.org/10.1016/j.ymssp.2018.12.032.
[11] Y.D. Ji, L. Zhang, M.K. Luo, Generalized stochastic resonance of power function type single-well system, Acta Phys. Sin. 63 (2014) 164302.
[12] Z.H. Lai, Y.G. Leng, S.B. Fan, Stochastic resonance of cascaded bistable duffing system, Acta Phys. Sin. 62 (2013) 070503.
[13] S.L. Lu, Q.B. He, J. Wang, A review of stochastic resonance in rotating machine fault detection, Mech. Syst. Signal Process. 116 (2019) 230–260.
[14] Z.J. Qiao, Y.G. Lei, J. Lin, S.T. Niu, Stochastic resonance subject to multiplicative and additive noise: the influence of potential asymmetries, Phys. Rev. E 94 (5) (2016) 052214.
[15] L. Zhang, W.B. Zheng, A.G. Song, Effect of the correlation between internal noise and external noise on logical stochastic resonance in bistable systems, Phys. Rev. E 96 (5) (2017) 052203.
[16] Z.H. Lai, Y.G. Leng, Dynamic response and stochastic resonance of tristable system, Acta Phys. Sin. 64 (2015) 200503.
[17] P.F. Xu, Y.F. Jin, S.M. Xiao, Stochastic resonance in a delayed triple-well potential driven by correlated noises, Chaos 27 (2017) 113109.
[18] D.Y. Han, P. Li, S.J. An, P.M. Shi, Multi-frequency weak signal detection based on wavelet transform and parameter compensation band-pass multi-stable stochastic resonance, Mech. Syst. Signal Process. 70–71 (2016) 995–1010.
[19] Y. Wang, S.B. Jiao, Q. Zhang, S. Lei, X.X. Qiao, A weak signal detection method based on adaptive parameter-induced tri-stable stochastic resonance, Chin. J. Phys. 56 (2018) 1187–1198.
[20] J.M. Li, X.F. Chen, Z.J. He, Multi-stable stochastic resonance and its application research on mechanical fault diagnosis, J. Sound Vibr. 332 (2013) 5999–6015.
[21] L.F. He, Y.Y. Cui, T.Q. Zhang, G. Zhang, Analysis of weak signal detection based on tri-stable system under Levy noise, Chin. Phys. B 25 (2016) 060501.
[22] H.K. Li, X.W. Zhang, C.B. He, F.J. Xu, X.F. Zhang, Weak fault enhancement method for blade crack by using stochastic resonance, J. Mech. Eng. 52 (2016)

94–101.
[23] H.B. Zhang, Q.B. He, S.L. Lu, F.R. Kong, Stochastic resonance with a joint woods-saxon and Gaussian potential for bearing fault diagnosis, Math. Probl. Eng. (2014) 315901.
[24] L.F. He, Y.Y. Cui, T.Q. Zhang, G. Zhang, Y. Song, Fault signal detection method based on power function type bistable stochastic resonance, Chin. J. Sci. Instrum. 37 (2016) 1457–1467.
[25] G. Zhang, J.P. Gao, Weak signal detection based on combination of power and exponential function model in tristable stochastic resonance, J. Comput. Appl. (2018) 1001–9081.
[26] Z.H. Zhang, D. Wang, T.Y. Wang, J.Z. Lin, Y.X. Jiang, Self-adaptive step-changed stochastic resonance using particle swarm optimization, J. Vibr. Shock 32 (2013) 125–130.
[27] J.M. Li, Y.G. Zhang, J.F. Zhang, P. Xie, Enhancement and extraction method of gear weak impact fault signal based on adaptive stochastic resonance, Acta Metrol. Sin. 38 (2017) 602–606.
[28] W.C. Cui, W. Li, F.L. Meng, L.M. Liu, Adaptive stochastic resonance method for bearing fault detection based on fruit fly optimization algorithm, J. Vibr. Shock 35 (2016) 96–100.
[29] Y.L. Wu, S.B. Jiao, Theory and Application of Brain Storm Optimization Algorithm, Science Press, Beijing, 2017, pp. 37–67.
[30] S.B. Jiao, C. Ren, W.C. Huang, Y.M. Liang, Stochastic resonance in an overdamped monostable system with multiplicative and additive α stable noise, Acta Phys. Sin. 62 (2013) 210501.
[31] L.Z. Zeng, R.H. Bao, B.H. Xu, Effects of Lévy noise in aperiodic stochastic resonance, J. Phys. A 40 (2007) 7175–7185.
[32] L.Z. Zeng, B.H. Xu, Effects of asymmetric Lévy noise in parameter-induced aperiodic stochastic resonance, Physica A 389 (2010) 5128–5136.